ACS OMEGA

http://pubs.acs.org/journal/acsodf

Article

Golden Glittering Biocomposite Fibers from Poly(lactic acid) and Nanosilver-Coated Titanium Dioxide with Unique Properties; Antimicrobial, Photocatalytic, and Ion-Sensing Properties

Kankavee Sukthavorn, Nollapan Nootsuwan, Ratthapit Wuttisarn, Suchada Jongrungruangchok, Chatchai Veranitisagul,* and Apirat Laobuthee*

Cite This: *ACS Omega* 2021, 6, 16307−16315

Read Online

ACCESS | Metrics & More | Article Recommendations

ABSTRACT: Golden glittering biocomposite fibers from poly(lactic acid) (PLA) and nanosilver-coated titanium dioxide (Ag/TiO_2) were successfully prepared *via* a melt spinning process. Various contents of 10% Ag/TiO_2/PLA masterbatch were diluted with PLA in concentrations of 5, 10, 15, 20, 25, and 30 phr, respectively. The physical, mechanical, thermal, and antibacterial properties of the obtained fibers were investigated. The results indicated that the glittering biocomposite fiber had a light, yellow-gold color and a slightly rough surface. Tenacity and elongation at break of the glittering biocomposite fibers were lower than those of the pristine PLA fiber. The thermal properties of the glittering composite fibers also decreased with increasing masterbatch content. The PLA/PEG-10 biocomposite fiber with good spinnability and mechanical properties was suitably used for preparing the golden glittering composite fabric by the knitting process. Moreover, the golden glittering biocomposite fabrics exhibited antibacterial activity against certain microbes, for example, *Staphylococcus aureus*, *Bacillus subtilis*, and *Candida albicans*. The prepared fabric has significant potential for use in eco-friendly textile products and antibacterial fabrics. Besides, our novel textiles showed not only the photocatalytic property needed to degrade organic dyes such as methylene blue in water but also the ion-sensing property for mercury(II) ions by changing the textile color from yellow to colorless.

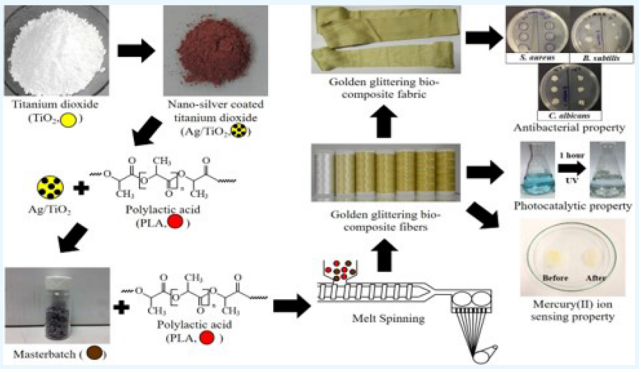

INTRODUCTION

In recent years, the development of textile products in the market has been achieved through the addition of specific properties or functions such as ultraviolet (UV) protection, antibacterial, stain-repellent, water-repellent, and antistatic textiles, and so forth to make textiles that achieve the interests and requirements of consumers, including making textile products to the point of being able to compete in the global market. Many researchers have, therefore, paid attention in developing novel textile products with special properties to fulfill the needs of many consumers and to improve the outdated textile technology to a more modern textile industry.

Titanium dioxide (TiO_2) is one of the interesting additives used for textile product development due to its non-toxicity, high chemical stability, good UV-blocking,[1] photocatalytic, and antibacterial properties.[2] Also, doping onto the TiO_2 with various metals, such as Ag, Au, Pt, Ru, Rh, and Pd, can enhance the efficiency of the photocatalytic and antibacterial properties of TiO_2, even in the absence of UV radiation.[3−6] Previously, our group successfully proposed and patented a new method to prepare silver nanoparticles using 3,4-dihydro-1,3,2*H*-benzoxazines (called as benzoxazine monomers) as a reducing agent. This method is remarkably simple and effective in terms of applying the silver nanoparticles on the surface of various materials, such as carbon black, silica (SiO_2), titanium dioxide (TiO_2), and so forth, in a matter of minutes.[7] Although this reducing method has many advantages, various organic solvents and benzoxazine monomers used in the preparation step can be toxic and expensive. Hence, our group has developed and patented a new and greener process for preparing the silver nanoparticles using water-soluble and non-toxic reducing agents such as ascorbic acid and water as a medium for coating silver nanoparticles onto material surfaces.[8] Besides, this green process provides silver-coated

Received: February 4, 2021
Accepted: June 9, 2021
Published: June 17, 2021

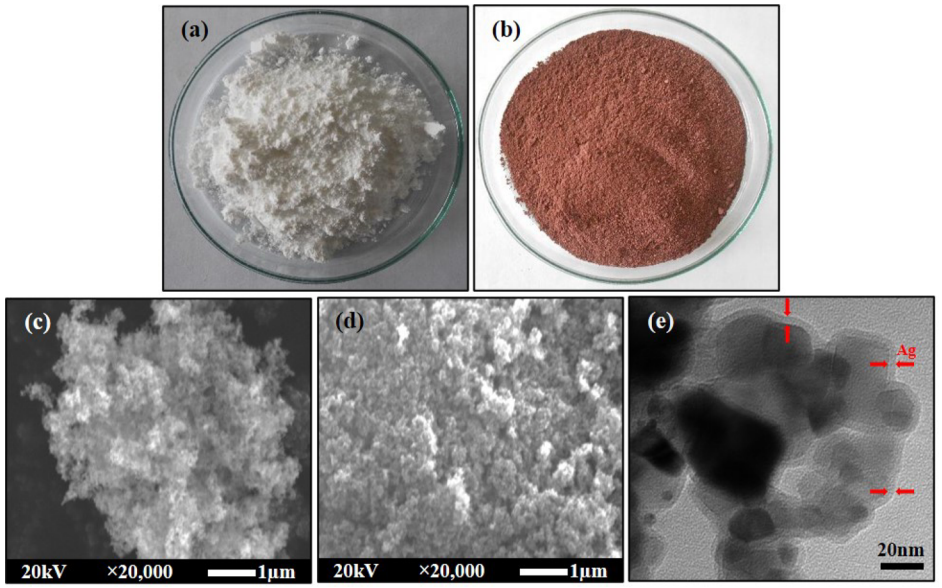

Figure 1. Physical appearances of (a) TiO_2 and (b) Ag/TiO_2; SEM images of (c) TiO_2 and (d) Ag/TiO_2; and (e) TEM image of Ag/TiO_2.

products as well as the process with benzoxazine monomers. Up to now, various antibacterial textiles and fabrics in the markets have been prepared by soaking in a solution with silver nanoparticles. The antibacterial properties of textiles or fabrics were reduced by washing several times, and the nanosilver particles cause pollution in wastewater. To solve this problem, the nanosilver particles should be incorporated into the textiles for long-lasting antibacterial properties and to prevent the loss of nanosilver particles during washing. A limitation is that the cost of nanosilver is high. Therefore, titanium dioxide with non-toxicity used as an additive in the textile industry was then used as a substrate for coating a small amount of nanosilver particles to enhance the antibacterial *via* our green process. The obtained nanosilver-coated titanium dioxide (Ag/TiO_2) was then prepared for achieving use as an antibacterial additive for polymer matrices in textile products.

To date, various research studies have focused on the use of poly(lactic acid) (PLA) instead of petroleum-based polymers since PLA is one of the biodegradable and environmentally friendly polymers with renewability, biodegradability, biocompatibility, and good thermomechanical properties.[9] Thus, PLA has been extensively used for medical, packaging, and textile applications. Although PLA shows strength, stiffness, and gas permeability properties, PLA still possesses limitations such as slow biodegradation rate, high cost, and low toughness.[10] Improving the toughness property of PLA has been suitably accomplished by blending PLA with other biobased polymers or plasticizers. Polyethylene glycol (PEG) is one of the interesting plasticizers used for PLA because of its non-toxicity, miscibility, and biodegradability. Also, PEG has been used to improve the ductility of PLA.[11]

To develop a novel biocomposite fiber with antibacterial properties, the prepared Ag/TiO_2 was used as an antibacterial additive and PEG was used as a plasticizer for PLA. Using the melt spinning technique, continuously long golden glittering biocomposite fibers were obtained for textile products. So far, no report exists on preparing golden glittering biocomposite fibers using our present method. In this work, the effect of Ag/TiO_2 loading on morphology, mechanical, thermal, and antibacterial properties was investigated. The obtained glittering composite fibers have been further used to prepare a prototype of the textile products *via* the knitting process. Degussa P25 as TiO_2 in this work showing the photocatalytic property to degrade organic compounds has been used for the wastewater treatment process in various industries. In practice, however, using TiO_2 powder for the wastewater treatment process has become a problem to remove TiO_2. To solve this problem, the use of TiO_2 was considered in the composite form. Not only were the results of the antibacterial property of our novel golden glittering biocomposite fibers consisting of Ag/TiO_2 shown in this work but also those of the photocatalytic property studied in our related studies have been introductorily presented. Since there are many studies that have reported on the interaction between mercury(II) ions and nanosilver detected by the change in color of nanosilver from yellow to colorless, here, the example of another application of our textiles as a mercury(II) ion sensor has been exhibited.[12]

RESULTS AND DISCUSSION

Characterization of Nanosilver-Coated Titanium Dioxide. The physical appearances of TiO_2 and Ag/TiO_2 are shown in Figure 1a,b, respectively. It was found that the color of TiO_2 powder changed from white to dark brown after coating with nanosilver particles. The scanning electron microscopy (SEM) image of TiO_2 (Figure 1c) illustrates the unclear shape and non-uniform size of TiO_2 particles with agglomeration. These results agreed with those reported by Hussain *et al.*[13] and Selvam and Swaminathan[14] about the aggregation and non-uniformity of TiO_2 (P25). Confirmed by SEM, Ag/TiO_2 particles also formed aggregation similarly to TiO_2 (Figure 1d). This result indicated that coating a small amount of Ag on the TiO_2 surface did not affect the aggregation of TiO_2 particles.

The transmission electron microscopy (TEM) image (Figure 1e) showed that in the morphology of Ag/TiO_2, two layers of nanoparticles were observed. The first layer was found to be an irregularly faceted morphology with an average diameter size of about 25 nm, which was assumed as a layer of TiO_2 corresponding to the research of Zuccheri *et al.*[15] The

https://doi.org/10.1021/acsomega.1c00657
ACS Omega 2021, 6, 16307−16315

second layer was found as a thin wall with a thickness size of about 7 nm covering TiO_2 particles and expected to be well-dispersed layers of silver nanoparticles on TiO_2 surfaces. The results confirmed that the efficient silver-coating process under green conditions developed by our group provided well-dispersed nanometallic silver on the particle supports as well as our previous process using benzoxazine monomers as a reducing agent.[7]

The specific surface area (S_{BET}) and average particle size (D_{BET}) of TiO_2 and Ag/TiO_2 powders are shown in Table 1. It was found that the S_{BET} of TiO_2 and Ag/TiO_2 powders was 76.70 and 77.77 m^2/g, respectively. The D_{BET} of TiO_2 and Ag/TiO_2 powders was 20.58 and 20.65 nm, respectively. It could be concluded that coating nanosilver on the surface of TiO_2 using this technique did not significantly affect the specific surface area of TiO_2.

Table 1. Specific Surface Area (S_{BET}), Density, and Average Particle Size (D_{BET}) of TiO_2 and Ag/TiO_2

samples	specific surface area; S_{BET} (m^2/g)	average particle size; D_{BET} (nm)
TiO_2	76.70	20.58
Ag/TiO_2	77.77	20.65

X-ray diffraction (XRD) measurement was used to investigate the effects of coating with nanosilver on the crystalline structures of the TiO_2. Figure 2a shows the XRD patterns of TiO_2 and Ag/TiO_2 powders. It was found that the XRD pattern of TiO_2 showed a mixture phase of anatase (JCPDS 01-089-4921) and rutile (JCPDS 01-086-0148). This agreed with the report of Selvum *et al.*[14] concerning a mixture phase of 80% anatase and 20% rutile in the XRD pattern of TiO_2 (P25). For Ag/TiO_2, it was found that the crystalline structure remained in the mixture phase between anatase and rutile. This suggests that the crystalline structure of TiO_2 was not affected by the nanosilver coating process used in this study. However, the XRD pattern of Ag/TiO_2 showed new weak peaks observed and assigned to the cubic metallic silver corresponding to the JCPDS 01-087-0720 standard. Cotolan *et al.*[16] explain that the presence of peaks for cubic crystalline silver proves the presence of silver within TiO_2 powder. The results by X-ray fluorescence (XRF) measurement, as shown in Figure 2b, revealed that elemental Ag appeared at around 6.27% and was well dispersed on the TiO_2 surface. These results also confirmed that the Ag species were successfully prepared.

The high-resolution XPS spectra of Ag 3d of Ag/TiO_2 powder are shown in Figure 2c. The XPS spectra of Ag 3d were found at 367.9 and 368.7 eV, which were attributed to Ag_2O and Ag^0, respectively. Xin *et al.*[17] and Zielińska *et al.*[18] found that the XPS spectra of Ag-doped TiO_2 showed a similar result at 367.7 and 368.2 eV and at 367.6 and 368.3 eV, attributed to Ag_2O and Ag^0, respectively. Moreover, the XPS spectra were also found at 369.8 eV, which was a similar result also found in research by Calderon *et al.*,[19] who found the XPS spectra at 369.4 eV and explained that the band to metallic sub-nanoparticles was associated with clusters smaller than 4 nm.

The antibacterial activity of TiO_2 and Ag/TiO_2 was investigated and confirmed by the inhibition zone appearing in Figure 2d. The results showed that TiO_2 (P25) did not exhibit an inhibition zone, while Ag/TiO_2 provided an inhibition zone for both bacteria [*Staphylococcus aureus* (*S. aureus*) and *Bacillus subtilis* (*B. subtilis*)]. The results concluded that by surface modification, TiO_2 can be modified as Ag/TiO_2 to enhance the antibacterial property.

Characterization of Golden Glittering Biocomposite Fibers and Fabrics. The physical appearance of the continuous PLA/PEG and glittering biocomposite fibers is shown in Figure 3a. It was found that the PLA/PEG fibers are glittering or glossy and colorless, resulting from the alignment of fibers in the machine direction from spinning and drawing processes. For glittering biocomposite fibers, they had a light

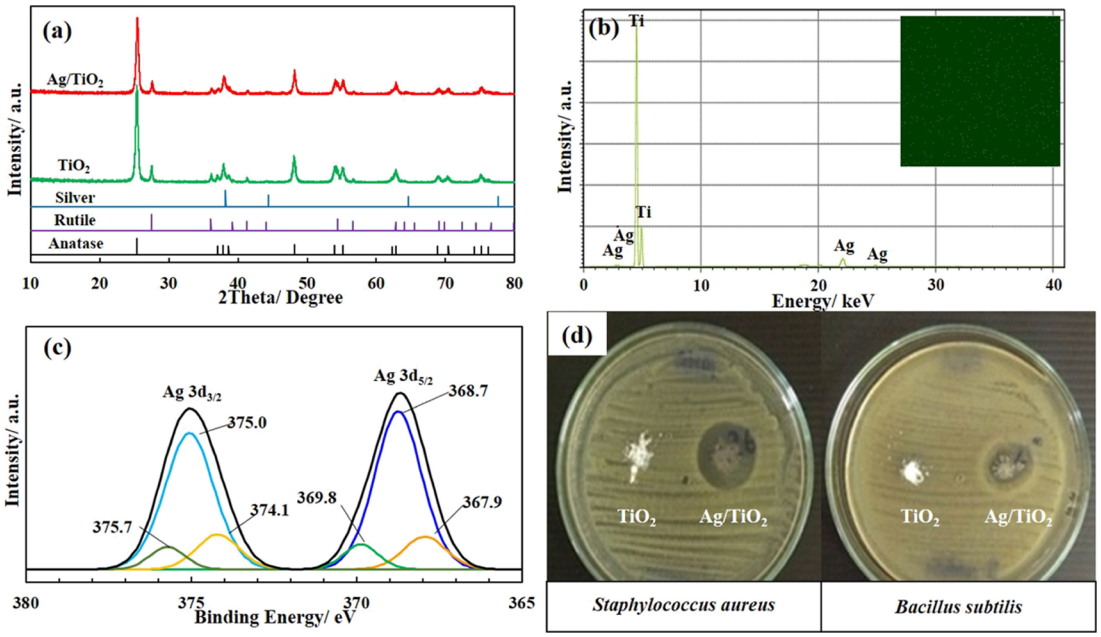

Figure 2. (a) XRD patterns, (b) XRF spectrum and mapping, and (c) high-resolution Ag 3d X-ray photoelectron spectroscopy (XPS) spectra of Ag/TiO_2 and (d) comparison of inhibition zones for TiO_2 and Ag/TiO_2 in Petri dishes.

https://doi.org/10.1021/acsomega.1c00657
ACS Omega 2021, 6, 16307−16315

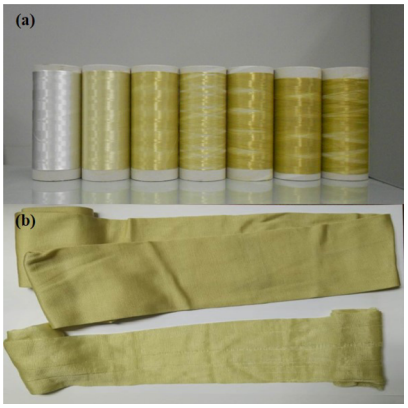

Figure 3. Physical appearances of (a) all glittering composite fibers and (b) PLA/PEG-10 fabric.

yellow-gold color to a dark yellow-gold color after adding higher masterbatch content. This yellow appearance may be caused by the interaction of light and conduction electrons around silver nanoparticles or localized surface plasmon resonance[20] or the spherical shape of nanosilver.[21] Moreover, Emam *et al.*[22] presented the coloration mechanism of yellow color viscose fibers using spherical Ag nanoparticles. The obtained fibers were successfully used to prepare a light yellow-gold color fabric *via* the circular knitting process, as shown in Figure 3b.

Tensile Measurement. The results of the tenacity and elongation at break of PLA/PEG fibers and all glittering biocomposite fibers are shown in Figure 4a,b, respectively. It was found that the tenacity of PLA/PEG, PLA/PEG-5, PLA/PEG-10, PLA/PEG-15, PLA/PEG-20, PLA/PEG-25, and PLA/PEG-30 was 3.71, 3.63, 3.34, 3.07, 3.15, 3.65, and 3.74 cN/tex, respectively (Figure 4a). It was revealed that the tendency of tenacity decreased with increasing masterbatch content. This might be due to that the Ag/TiO_2 formed the large agglomerates in the PLA matrix, leading to generate some defects inside the PLA fiber during fiber forming. Besides, by adding a high concentration of Ag/TiO_2, the poor spinnability of the glittering biocomposite fiber was obtained. Feng *et al.*[23] and Athanasoulia *et al.*[24] found that adding a high concentration of TiO_2 resulted in decreasing the tensile strength and elongation at break.

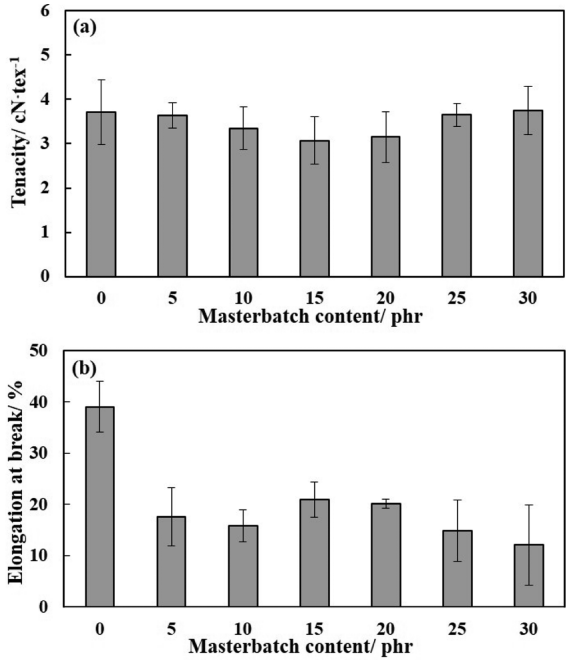

Figure 4. (a) Tenacity and (b) elongation at break of PLA/PEG fibers and glittering composite fibers.

Elongation at break of PLA/PEG was 39.04%, while elongation at break of PLA/PEG-5, PLA/PEG-10, PLA/PEG-15, PLA/PEG-20, PLA/PEG-25, and PLA/PEG-30 was 17.61, 15.85, 21.00, 20.16, 14.92, and 12.08%, respectively (Figure 4b). Therefore, the tendency of elongation at break decreased with increasing masterbatch content. It might be due to the rigidity of the Ag/TiO_2 filler. There is no elongation while applying tension, so the elongation at break declined with an increase in Ag/TiO_2. This is consistent with the report of Wu *et al.*,[25] which showed that elongation at break decreased with increasing nano-SiO_2 contents in the PLA filament.

XRD Measurement. XRD patterns of PLA/PEG fibers and glittering composite fibers are shown in Figure 5. A broad peak around 17.00° of PLA/PEG fibers was observed, as previously presented by Chieng *et al.*[26] For the glittering biocomposite fibers, it was found that the two weak peaks around 25.48 and 29.28° corresponded to the anatase and rutile phases, respectively. The peak of the rutile phase shifted slightly from 27.59 to 29.28°. The intensity diffraction peak increased with increasing Ag/TiO_2 content.

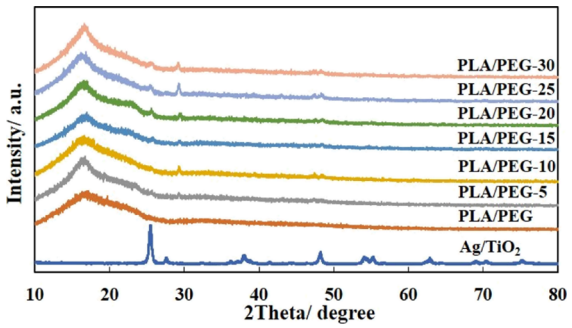

Figure 5. XRD patterns of Ag/TiO_2, PLA/PEG fibers, and glittering composite fibers.

Morphology. The surface morphology of PLA/PEG fibers and glittering biocomposite fibers filled with various contents of masterbatches is shown in Figure 6. It was found that the PLA/PEG fiber had a smooth surface due to homogeneous mixing between PLA and PEG, with a diameter of the fiber of about 50 μm (Figure 6a).[27] For the glittering biocomposite fibers, it was found that there was slight roughness on the surface with increasing masterbatch content, with a diameter of the fiber of about 30−50 μm (Figure 6b−g). Moreover, SEM images do not find the larger aggregation of Ag/TiO_2 on the surface of fibers due to good dispersion and the distribution of Ag/TiO_2 in the PLA matrix.[28]

Thermal Properties. Figure 7 shows the differential scanning calorimetry (DSC) thermograms of PLA/PEG fibers and glittering biocomposite fibers; the calorimetric parameters are summarized in Table 2. Glass transition temperature (T_g) of the PLA/PEG fiber was 60.8 °C, while that of the masterbatch of Ag/TiO_2 was decreased from 59.6 to 50.2 °C with an increase in the content of Ag/TiO_2. Similar results

https://doi.org/10.1021/acsomega.1c00657
ACS Omega 2021, 6, 16307−16315

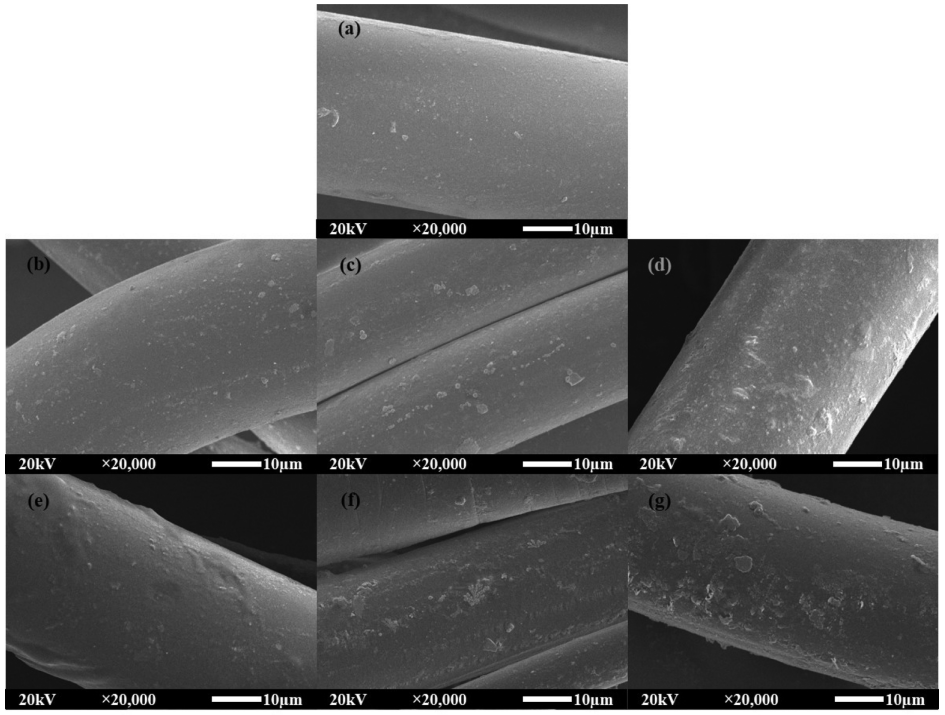

Figure 6. SEM images of (a) PLA/PEG fibers and glittering composite fibers with masterbatch content at (b) 5, (c) 10, (d) 15, (e) 20, (f) 25, and (g) 30 phr.

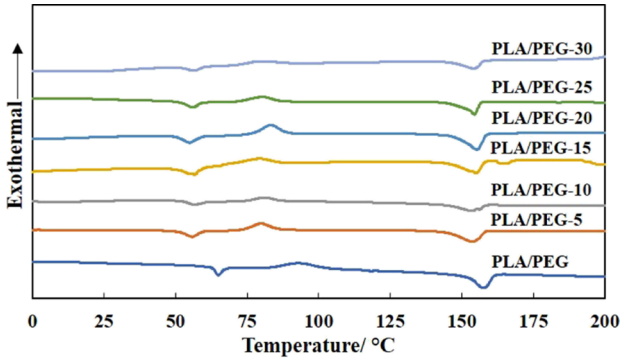

Figure 7. DSC thermograms of PLA/PEG fibers and glittering composite fibers.

Table 2. Thermal Parameters from DSC for PLA/PEG Fibers and Golden Glittering Biocomposite Fibers

	temperature (°C)					
samples	T_g	T_c	T_m	ΔH_c (J/g)	ΔH_m (J/g)	X_c (%)
PLA/PEG	60.82	93.14	157.32	20.28	29.18	10.56
PLA/PEG-5	55.78	79.83	153.40	17.55	32.25	17.45
PLA/PEG-10	52.31	81.00	153.26	15.29	26.77	13.62
PLA/PEG-15	56.63	78.86	154.95	29.72	36.32	7.83
PLA/PEG-20	54.95	83.19	155.06	22.34	36.69	17.03
PLA/PEG-25	50.19	80.46	154.19	15.70	27.11	13.54
PLA/PEG-30	59.55	79.54	154.02	17.60	28.34	12.74

were also found in the research of Farhoodi *et al.*,[29] who explained that the agglomeration of nanoparticles could disturb the arrangement of polymer chains and cause free volume increment, resulting in the decrement of T_g.

The crystallization temperature (T_c) of the PLA/PEG fiber was 93.1 °C. The more increased the masterbatch contents, the lower the tendency of crystallization temperature obtained from 83.1 to 78.9 °C. This might be due to Ag/TiO_2 being able to act as a nucleating agent; it could also retard crystallization from the melting state.[30] Crystallinity (X_c) of the PLA/PEG fiber was found to be 10.6%. Increasing the masterbatch contents showed a slight increment of crystallinity. This might be due to the good dispersion of Ag/TiO_2 into the matrix by adding low masterbatch contents. Moreover, Ag/TiO_2 might act as a nucleating agent to increase the crystallinity of the composites.

The melting temperature (T_m) of the PLA/PEG fiber was 157.3 °C, while the melting temperature of the masterbatches decreased from 155.1 to 153.3 °C with increasing Ag/TiO_2 content. This agrees with the results presented by Mallick *et al.*,[31] who reported that the TiO_2 nanoparticles obstructed the regularity of the PLA chain structures and increased the free volume between the molecular chains, resulting in the decrement of the melting temperature.

Antibacterial Property of Golden Glittering Biocomposite Fabrics. The antibacterial ability of the glittering biocomposite fabrics was investigated by observing the survival of Gram-positive bacteria (*S. aureus* and *B. subtilis*) and the fungus [*Candida albicans* (*C. albicans*)] under an incubation time, as presented in Figure 8a. Here, PLA/PEG-10 biocomposite fibers were used to prepare PLA/PEG-10 composite fabrics, as these fibers consisted of the upper limit of Ag/TiO_2 content still showing a light yellow-gold color and a good spinnability. The results showed that PLA/PEG-10 composite fabrics could inhibit the bacterial growth of *S. aureus*, *B. subtilis*, and *C. albicans* up to 70.49, 88.89, and 46.15%, respectively. Moreover, the population of Gram-positive bacteria shows a significant percentage reduction more than that of fungus for the entire incubation time. This result

https://doi.org/10.1021/acsomega.1c00657
ACS Omega 2021, 6, 16307−16315

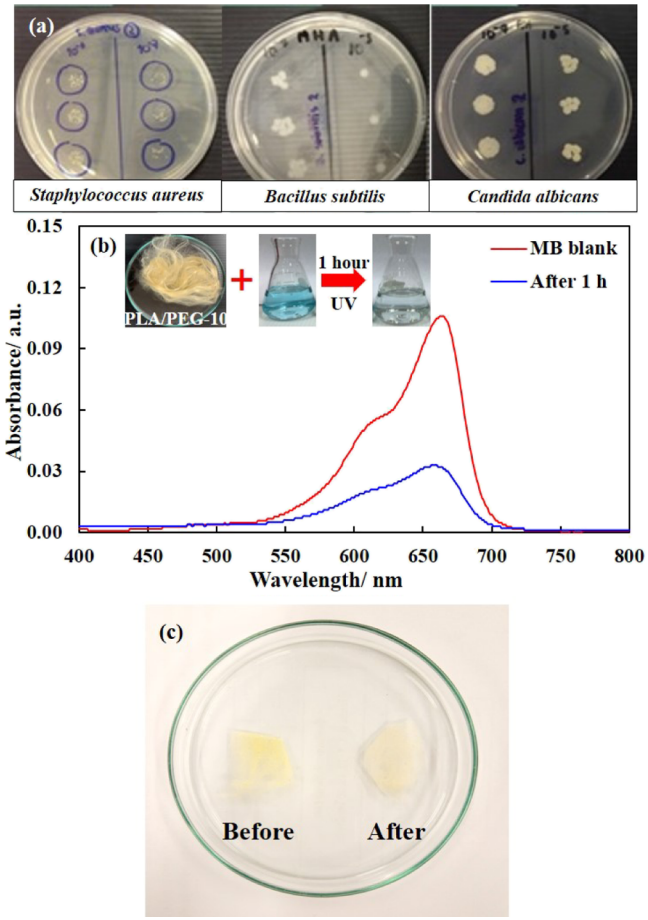

Figure 8. (a) Antimicrobial property of the PLA/PEG-10 fabric, (b) UV−visible (UV−vis) absorption spectra of MB dye before and after under UV irradiation *via* a photocatalytic property of PLA/PEG-10 fibers, and (c) colorimetric sensing property of PLA/PEG-10 fibers in the mercury ion solution, before and after 24 h.

revealed that the Ag/TiO_2 particles dispersed within the PLA matrix and acted as an antibacterial agent for the textile product, especially for inhibiting the growth of Gram-positive bacteria.

Photocatalytic and Mercury(II) Ion-Sensing Properties of PLA/PEG-10 Fibers. The preliminary results of the photocatalytic and mercury(II) ion-sensing properties of PLA/PEG-10 fibers were also presented in this work. The photocatalytic properties of PLA/PEG-10 fibers were used to degrade methylene blue (MB) as a model dye under UV irradiation. By calculation, the PLA/PEG-10 fibers used in this study consisted of a matrix at around 99.09 wt % and filler at around 0.91 wt %, which is composed of Ag and TiO_2 at 0.057 and 0.853%, respectively. The PLA/PEG-10 fibers could be reused to degrade MB in up to three cycles with the percentage of degradation around 60% (Figure 8b), while Ag/TiO_2 powder could degrade MB 100%. The results illustrated that the photocatalytic efficiency of Ag/TiO_2 decreased when the Ag/TiO_2 powder was used as an additive. Some part of the Ag/TiO_2 surface was covered by the PLA matrix, resulting in the decrement of the surface area of Ag/TiO_2 to degrade MB. However, using the composite fibers provided the advantage of easily removing the photocatalysts after use. In our related studies, the glittering biocomposite fibers and membranes have been used to study the photocatalytic activity with organic dyes in water.

Figure 8c shows an image of the glittering biocomposite fiber before and after testing of mercury(II) ion sensing. The colorimetric sensing of mercury(II) ions was carried out by immersing glittering biocomposite fibers into a mercury solution. After 24 h, it was found that the glittering biocomposite fibers changed from a light yellow-gold color to colorless. Similar results were also found in research by Jeevika and Shankaran,[12] who found that the color of the AgNP/poly(vinyl alcohol) nanocomposite hydrogel changed from yellow to colorless. The results also implied that the glittering biocomposite fibers can be used as a colorimetric sensor for mercury(II) ions. In our related studies, the glittering biocomposites have been prepared as the fiber and membrane forms for use as the colorimetric sensors for mercury(II) ions and other transition or rare-earth metal ions.

CONCLUSIONS

Nanosilver-coated titanium dioxide was successfully prepared using ascorbic acid as a reducing agent and used as filler in PLA/PEG to prepare glittering biocomposite fibers. By increasing the masterbatch content, the yellow-gold color of the glittering biocomposite fibers changed from light to dark, while tenacity and elongation at break of these fibers decreased. For the thermal properties of the glittering biocomposite fibers, it was found that the glass transition temperatures, crystallization temperatures, and melting temperatures of all fibers decreased with increasing crystallinity compared to those of PLA/PEG fibers. Moreover, PLA/PEG-10 consisted of the highest Ag/TiO_2 content that could still have a light yellow-gold color, have good spinnability, and have suitable mechanical and thermal properties for preparing glittering biocomposite fabrics. The PLA/PEG-10 also showed antibacterial activity against certain microbes, especially Gram-positive bacteria. The prepared fabrics have significant potential for use as an eco-friendly textile product with antibacterial properties. Moreover, these novel fibers with the photocatalytic ability to degrade organic dyes and the mercury(II) ion-sensing property by changing the color of fibers should be considered as photocatalytic materials for wastewater treatment and as mercury(II) ion sensors in near future.

EXPERIMENTAL SECTION

Materials. Commercial titanium dioxide (TiO_2, Degussa P25), with an anatase−rutile crystalline mixed phase, was purchased from Evonik Industries, USA. Silver nitrate ($AgNO_3$, analytical reagent grade) was purchased from POCH Company, Poland. Ascorbic acid ($C_6H_8O_6$, analytical grade) was purchased from Daejung Chemical & Metals Company, Korea. PLA (grade 3052D) was purchased from NatureWorks LLC, USA. PEG (MW = 4000) was purchased from Ajax Finechem Pty Ltd, Australia.

Preparation and Characterization of Nanosilver-Coated Titanium Dioxide. Nanosilver-coated titanium dioxide (Ag/TiO_2) was successfully prepared according to Lertprapaporn *et al.*[8] and Thai petty patent no. 15514. A total of 50 g of titanium dioxide, 5% by mole of silver nitrate, and distilled water were added to a beaker and stirred at room temperature for 15 min, and then, 5% by mole of ascorbic acid as a reducing agent was added into the beaker. Then, the

https://doi.org/10.1021/acsomega.1c00657
ACS Omega 2021, 6, 16307−16315

mixture was stirred at room temperature for 2 h. The product was washed with distilled water, filtered by vacuum filtration, and dried at 60 °C for 24 h to obtain the Ag/TiO_2 powder.

The surface morphology of Ag/TiO_2 was studied by SEM (JEOL, JSM-6510) with an acceleration voltage of 10 kV.

A high-resolution image of the Ag/TiO_2 was studied by TEM (Hitachi HT 7700) with 120 kV accelerating voltage.

The density of the Ag/TiO_2 was characterized using a density analyzer (Pycnometer, AccuPyc 1330) with helium gas for the open/close cell.

Specific surface area (S_{BET}) measurement was carried out using Brunauer−Emmett−Teller (BET) analysis by nitrogen adsorption isotherm using a Micromeritics (Quantachrome, Autosorb 1). The S_{BET} was calculated into the average particle size (D_{BET}) according to the formula given below[32]

$$D_{BET} = 6000/(d_{th} \times S_{BET}) \quad (1)$$

where D_{BET} is the average particle size (nm), S_{BET} is a specific surface area (m^2/g), and d_{th} is the theoretical density of the materials (g/cm^3).

The phase and structure of the Ag/TiO_2 were characterized using an X-ray diffractometer (X'PertPRO MPD diffractometer) operating at 40 kV and 30 mA. The scanning rate was 0.02°/min in the 2θ diffraction angles ranging from 10 to 80°.

The chemical compositions of the Ag/TiO_2 were characterized by XRF spectroscopy (Horiba XGT-2000W) with the X-ray tube operated at 50 kV and 1 mA.

XPS measurements were performed on an X-ray photoelectronic spectrometer (Kratos; Axis Ultra DLD), employed to identify the valence states of Ag.

The antibacterial properties of Ag/TiO_2 were studied by an agar disc diffusion method. The Gram-positive bacteria used in this study were *S. aureus* (ATCC 25923) and *B. subtilis* (ATCC 6633). All bacteria were incubated at 37 °C for 24 h. The efficiency of the antibacterial properties was evaluated from the diameter of the inhibition zone for each sample.

Preparation of Composite Golden Glittering Biocomposite Fibers and Fabrics. PLA pellets and the nanosilver-coated titanium dioxide (Ag/TiO_2) were dried in an oven at 60 °C for 24 h before processing to avoid the moisture generation during the melt processing. PLA and 10 wt % of Ag/TiO_2 were mixed and extruded in a twin-screw extruder at a temperature between 150 and 180 °C to obtain the masterbatch pellets. The masterbatch and PLA pellets were dried in an oven at 60 °C for 24 h before processing. The masterbatch, PLA pellets, and PEG were mixed according to the compositions in Table 3; the mixture was melt-extruded using a single-screw extruder with a 24-hole spinneret and a diameter size of 0.32 mm, spinning temperature between 190 and 220 °C, screw speed of 8 rpm, and free fall at draw speed of 500 m/min for spinning the glittering biocomposite fibers. This parameter is developed and modified from the studies in the literature of Pivsa-Art *et al.*[33] and Prahsarn *et al.*[34] During spinning, it was observed that to evaluate fiber spinnability, the continuous and steady spinning of fibers without breakage was regarded as good fiber spinnability. The nomenclature and spinnability of the glittering biocomposite fibers are given in Table 3. The glittering biocomposite fibers were also used to make the prototype of glittering biocomposite fabrics using a circular knitting machine. The glittering biocomposite yarn was fed to the needle and knitted into stockings or socks, with an overfeed at 85% and a speed of rotation of about 10 rpm.

Table 3. Compositions and Spinnability of PLA, PEG, and Masterbatch of Ag/TiO_2 in Composite Fibers

	matrix (wt %)			
code	PLA	PEG	masterbatch of Ag/TiO_2 (phr)	spinnability
PLA/PEG	90	10	0	good
PLA/PEG-5	90	10	5	good
PLA/PEG-10	90	10	10	better
PLA/PEG-15	90	10	15	better
PLA/PEG-20	90	10	20	poor
PLA/PEG-25	90	10	25	poor
PLA/PEG-30	90	10	30	poor

Characterization of Golden Glittering Biocomposite Fibers and Fabrics. The tensile test for the glittering biocomposite fibers was performed using a universal testing machine (Instron-5944) with a gauge length of 25 mm, 30 mm/min elongation rate, and a 10 N load cell according to the standard testing method: ASTM D3822.

Phase identification of the glittering biocomposite fibers was performed on an X-ray diffractometer (X'PertPRO) operating at 40 kV and 30 mA; the scanning rate was 0.02°/min in the 2θ diffraction angle from 10 to 80°.

The surface morphology of the glittering biocomposite fibers was characterized on a scanning electron microscope (JEOL, JSM-6510) operating at an accelerating voltage of 5 kV. The surface of fibers was coated with a thin layer of gold to avoid image distortion due to charging.

Glass transition temperature (T_g), crystallization temperature (T_c), and melting temperature (T_m) of glittering biocomposite fibers were characterized on a differential scanning calorimeter (Mettler Toledo, DSC1) in a temperature range of 0−200 °C and a heating rate of 10 °C/min under a nitrogen atmosphere.

The antibacterial properties of glittering biocomposite fabrics were measured according to the standard of ASTM E2149-01. The bacteria used in this study were Gram-positive bacteria, *S. aureus* and *B. subtilis*, including the fungus *C. albicans*. The efficiency of the antibacterial properties was calculated from the percent reduction of bacteria according to the formula given below

$$\text{Reduction of bacteria } (\%) = (B - A) \times 100/B \quad (2)$$

where A is the number of bacteria recovered after the dynamic contact of the sample at the time of 24 h and B is the number of bacteria before the addition of the sample at time 0 h.

A preliminary study on the photocatalytic property and mercury(II) ion-sensing property of glittering biocomposite textiles was also presented.

The solution of MB dye was prepared from 1 ppm dye in water. A total of 0.3 g of PLA/PEG-10 fibers was dispersed into 20 mL of dye. After irradiation under UV for 60 min, the dye solution was investigated for photocatalytic degradation using UV−vis absorption spectroscopy.

$$\text{Percentage of degradation } (\%) = (A_o - A_t)/A_o \times 100 \quad (3)$$

where A_o is the initial concentration of MB and A_t is the concentration of MB after illumination at time t.

The solution of mercury was prepared from 5% w/v of mercury chloride in water. Then, the glittering biocomposite

https://doi.org/10.1021/acsomega.1c00657
ACS Omega 2021, 6, 16307−16315

fibers were soaked in 50 mL of mercury solution. The change in the color of the glittering biocomposite fibers was observed.

AUTHOR INFORMATION

Corresponding Authors

Chatchai Veranitisagul − *Department of Materials and Metallurgical Engineering, Faculty of Engineering, Rajamangala University of Technology Thanyaburi, Pathumthani 12110, Thailand*; Email: chatchai.v@en.rmutt.ac.th

Apirat Laobuthee − *Department of Materials Engineering, Faculty of Engineering, Kasetsart University, Bangkok 10900, Thailand*; orcid.org/0000-0001-9744-9864; Email: fengapl@ku.ac.th

Authors

Kankavee Sukthavorn − *Department of Materials Engineering, Faculty of Engineering, Kasetsart University, Bangkok 10900, Thailand*

Nollapan Nootsuwan − *Department of Materials Engineering, Faculty of Engineering, Kasetsart University, Bangkok 10900, Thailand*

Ratthapit Wuttisarn − *Department of Materials Engineering, Faculty of Engineering, Kasetsart University, Bangkok 10900, Thailand*

Suchada Jongrungruangchok − *Department of Pharmaceutical Chemistry, Faculty of Pharmacy, Rangsit University, Pathumthani 12000, Thailand*

Complete contact information is available at: https://pubs.acs.org/10.1021/acsomega.1c00657

Notes

The authors declare no competing financial interest.

ACKNOWLEDGMENTS

The authors would like to thank PTT Public Company Limited for its financial support under the research funding topic "Green and Sustainable Polymers: A Challenge for Renewable Resource-Rich Thailand". The authors would also like to thank the Department of Textile Engineering of the Faculty of Engineering at the Rajamangala University of Technology Thanyaburi for allowing the use of its processing machines.

REFERENCES

(1) Yang, H.; Zhu, S.; Pan, N. Study on Mechanisms of Titanium Dioxide as Ultraviolet-Blocking Additive for Films and Fabrics by an Improved Scheme. *J. Appl. Polym. Sci.* **2004**, *92*, 3201−3210.

(2) Kaseem, M.; Hamad, K.; Ur Rehman, Z. Review of Recent Advances in Polylactic Acid/TiO_2 Composites. *Materials* **2019**, *12*, 3659.

(3) Jakob, M.; Levanon, H.; Kamat, P. V. Charge Distribution between UV-Irradiation TiO_2 and Gold Nanoparticles: Determination of Shift in the Fermi Level. *Nano Lett.* **2003**, *3*, 353−358.

(4) Pant, H. R.; Pandeya, D. R.; Nam, K. T.; Baek, W.-i.; Hong, S. T.; Kim, H. Y. Photocatalytic and Antibacterial Properties of a TiO_2/Nylon-6 Electrospun Nanocomposite Mat Containing Silver Nanoparticles. *J. Hazard. Mater.* **2011**, *189*, 465−471.

(5) Shang, L.; Li, B.; Dong, W.; Chen, B.; Li, C.; Tang, W.; Wang, G.; Wu, J.; Ying, Y. Heteronanostructure of Ag Particle on Titanate Nanowire Membrane with Enhanced Photocatalytic Properties and Bactericidal Activities. *J. Hazard. Mater.* **2010**, *178*, 1109−1114.

(6) Cheng, B.; Le, Y.; Yu, J. Preparation and Enhanced Photocatalytic Activity of Ag@TiO_2 Core-Shell Nanocomposite Nanowires. *J. Hazard. Mater.* **2010**, *177*, 971−977.

(7) Kaewvilai, A.; Wattanathana, W.; Jongrungruangchok, S.; Veranitisagul, C.; Koonsaeng, N.; Laobuthee, A. 3,4-Dihydro-1,3-2H-benzoxazines: Novel Reducing Agents through One Electron Donation Mechanism and Their Application as the Formation of Nano-Metallic Silver Coating. *Mater. Chem. Phys.* **2015**, *167*, 9−13.

(8) Lertprapaporn, T.; Manuspiya, H.; Laobuthee, A. Dielectric Improvement from Novel Polymeric Hybrid Films Derived by Polylactic acid/Nanosilver Coated Microcrystalline Cellulose. *Mater. Today* **2018**, *5*, 9326−9335.

(9) Raquez, J.-M.; Habibi, Y.; Murariu, M.; Dubois, P. Polylactic Acid (PLA) based Nanocomposites. *Prog. Polym. Sci.* **2013**, *38*, 1504−1542.

(10) Hamad, K.; Kaseem, M.; Ayyoob, M.; Joo, J.; Deri, F. Polylactic acid Blend: the Future of Green, Light and Tough. *Prog. Polym. Sci.* **2018**, *85*, 83−127.

(11) Li, D.; Jiang, Y.; Lv, S.; Liu, X.; Gu, J.; Chen, Q.; Zhang, Y. Preparation of Plasticized Poly (Lactic Acid) and Its Influence on the Properties of Composite Materials. *PLoS One* **2018**, *13*, No. e0193520.

(12) Jeevika, A.; Shankaran, D. R. Functionalized Silver Nanoparticles Probe for Visual Colorimetric Sensing of Mercury. *Mater. Res. Bull.* **2016**, *83*, 48−55.

(13) Hussain, M.; Ceccarelli, R.; Marchisio, D. L.; Fino, D.; Russo, N.; Geobaldo, F. Synthesis, Characterization, and Photocatalytic Application of Novel TiO_2 Nanoparticles. *Chem. Eng. J.* **2010**, *157*, 45−51.

(14) Selvam, K.; Swaminathan, M. Photocatalytic Synthesis of 2-Methylquinolines with TiO_2 Wackherr and Home Prepared TiO_2 − a Comparative Study. *Arabian J. Chem.* **2017**, *10*, S28−S34.

(15) Zuccheri, T.; Colonna, M.; Stefanini, I.; Santini, C.; Gioia, D. Bactericidal Activity of Aqueous Acrylic Paint Dispersion for Wooden Substrates Based on TiO_2 Nanoparticles Activated by Fluorescent Light. *Materials* **2013**, *6*, 3270−3283.

(16) Cotolan, N.; Rak, M.; Bele, M.; Cör, A.; Muresan, L. M.; Milošev, I. Sol-gel Synthesis, Characterization and Properties of TiO_2 and Ag-TiO_2 Coatings on Titanium Substrate. *Surf. Coat. Technol.* **2016**, *307*, 790−799.

(17) Xin, B.; Jing, L.; Ren, Z.; Wang, B.; Fu, H. Effect of Simultaneously Doped and Deposited Ag on the Photocatalytic Activity and Surface State of TiO_2. *J. Phys. Chem. B* **2005**, *109*, 2805−2809.

(18) Zielińska, A.; Kowalska, E.; Sobczak, J. W.; Łącka, I.; Gazda, M.; Ohtani, B.; Hupka, J.; Zaleska, A. Silver-Doped TiO_2 Prepared by Microemulsion Method: Surface Properties, Bio-and Photoactivity. *Sep. Purif. Technol.* **2010**, *72*, 309−318.

(19) Calderon, S. V.; Galindo, R. E.; Benito, N.; Palacio, C.; Cavaleiro, A.; Carvalho, S. Ag^+ Release Inhibition from ZrCN-Ag Coatings by Surface Agglomeration Mechanism: Structural Characterization. *J. Phys. D: Appl. Phys.* **2013**, *46*, 325303.

(20) Jafari, N.; Karimi, L.; Mirjalili, M.; Derakhshan, S. J. Effect of Silver Particle Size on Color and Antibacterial Properties of Silk and Cotton Fabrics. *Fibers Polym.* **2016**, *17*, 888−895.

(21) Abdel-Mohsen, A. M.; Abdel-Rahman, R. M.; Fouda, M. M. G.; Vojtova, L.; Uhrova, L.; Hassan, A. F.; Al-Deyab, S. S.; El-Shamy, I. E.; Jancar, J. Preparation, Characterization and Cytotoxicity of Schizophyllan/Silver Nanoparticle Composite. *Carbohydr. Polym.* **2014**, *102*, 238−245.

(22) Emam, H. E.; Mowafi, S.; Mashaly, H. M.; Rehan, M. Production of Antibacterial Colored Viscose Fibers Using in Situ Prepared Spherical Ag Nanoparticles. *Carbohydr. Polym.* **2014**, *110*, 148−155.

(23) Feng, S.; Zhang, F.; Ahmed, S.; Liu, Y. Physico-Mechanical and Antibacterial Properties of PLA/TiO_2 Composite Materials Synthesized via Electrospinning and Solution Casting Process. *Coatings* **2019**, *9*, 525.

(24) Athanasoulia, I.-G.; Mikropoulou, M.; Karapati, S.; Tarantili, P.; Trapalis, C. Study of Thermomechanical and Antibacterial Properties of TiO_2/Poly(Lactic Acid) Nanocomposites. *Mater. Today* **2018**, *5*, 27553−27562.
(25) Wu, G.; Liu, S.; Jia, H.; Dai, J. Preparation and Properties of Heat Resistant Polylactic Acid (PLA)/Nano-SiO_2 Composite Filament. *J. Wuhan Univ. Technol., Mater. Sci. Ed.* **2016**, *31*, 164−171.
(26) Chieng, B. W.; Ibrahim, N. A.; Yunus, W. M. Z. W.; Hussein, M. Z. Poly(Lactic Acid)/Poly(Ethylene Glycol) Polymer Nanocomposites: Effects of Graphene Nanoplatelets. *Polymers* **2014**, *6*, 93−104.
(27) Hossain, K. M. Z.; Parsons, A. J.; Rudd, C. D.; Ahmed, I.; Thielemans, W. Mechanical, Crystallization and Moisture Absorption Properties of Melt Drawn Polylactic Acid Fibers. *Eur. Polym. J.* **2014**, *53*, 270−281.
(28) Mujica-Garcia, A.; Hooshmand, S.; Skrifvars, M.; Kenny, J. M.; Oksman, K.; Peponi, L. Poly(Lactic Acid) Melt-Spun Fibers Reinforced with Functionalized Cellulose Nanocrystals. *RSC Adv.* **2016**, *6*, 9221−9231.
(29) Farhoodi, M.; Dadashi, S.; Mousavi, S. M. A.; Sotudeh-Gharebagh, R.; Emam-Djomeh, Z.; Oromiehie, A.; Hemmati, F. Influence of TiO_2 Nanoparticle Filler on the Properties of PET and PLA Nanocomposites. *Polymer* **2012**, *36*, 745−755.
(30) Nomai, J.; Suksut, B.; Schlarb, A. K. Crystallization Behavior of Poly(Lactic Acid)/Titanium Dioxide Nanocomposites. *KMUTNB Int. J. Appl. Sci. Technol.* **2015**, *8*, 251−258.
(31) Mallick, S.; Ahmad, Z.; Touati, F.; Bhadra, J.; Shakoor, R. A.; Al-Thani, N. J. PLA-TiO_2 Nanocomposites: Thermal, Morphological, Structural, and Humidity Sensing Properties. *Ceram. Int.* **2018**, *44*, 16507−16513.
(32) Wattanathana, W.; Nootsuwan, N.; Veranitisagul, C.; Koonsaeng, N.; Laosiripojana, N.; Laobuthee, A. Simple Cerium-Triethanolamine Complex: Synthesis, Characterization, Thermal Decomposition and Its Application to Prepare Ceria Support for Platinum Catalysts Used in Methane Steam Reforming. *J. Mol. Struct.* **2015**, *1089*, 9−15.
(33) Pivsa-Art, S.; Srisawat, N.; O-Charoen, N.; Pavasupree, S.; Pivsa-Art, W. Preparation of Knitting Socks from Poly (lactic acid) and Poly[(*R*)-3-hydroxybutyrate-*co*-(*R*)-3-hydroxyvalerate] (PHBV) blends for Textile Industrials. *Energy Procedia* **2011**, *9*, 589−597.
(34) Prahsarn, C.; Sooksimuang, T.; Sahasithiwat, S.; Roungpaisan, N.; Kamtonwong, S.; Panchan, W.; Klinsukhon, W.; Suwannamek, N. Luminescent Polypropylene Fibers containing Novel Organic Luminescent Substance. *J. Polym. Res.* **2015**, *22*, 87.

https://doi.org/10.1021/acsomega.1c00657
ACS Omega 2021, 6, 16307−16315